2019 IEEE International Ultrasonics Symposium (IUS)
Glasgow, Scotland, October 6-9, 2019

A Spatially Weighted Regularization Method for Attenuation Coefficient Estimation

Farah Deeba*, Ricky Hu*, Jefferson Terry†, Denise Pugash‡, Jennifer A. Hutcheon§, Chantal Mayer1§, Septimiu Salcudean*, and Robert Rohling*¶
*Department of Electrical and Computer Engineering, University of British Columbia, Vancouver, British Columbia, Canada
†Department of Pathology and Laboratory Medicine, University of British Columbia, Vancouver, British Columbia, Canada
‡Department of Radiology, University of British Columbia, Vancouver, British Columbia, Canada
§Department of Obstetrics and Gynaecology, University of British Columbia, Vancouver, British Columbia, Canada
¶Department of Mechanical Engineering, University of British Columbia, Vancouver, British Columbia, Canada
Email: {rohling, farahdeeba}@ece.ubc.ca

***Abstract*—Existing methods for measuring the ultrasonic attenuation coefficient estimate (ACE) fail to take into account the effect of tissue heterogeneity. We propose a total variation (TV) regularization based method, where the local regularization will be modulated as a function of envelope signal-to-noise-ratio deviation, an indicator of tissue heterogeneity. We evaluate our approach using three physical phantoms with different configurations. We also demonstrate the application of the method for placenta *ex vivo*. The proposed method results in significant improvement in ACE measurement compared to the reference phantom method for all the experiments. Specifically, the method shows promising results in the presence of heterogeneity, exceeding the performance of both reference phantom and unweighted total variation regularization in terms of accuracy, precision and resolution-precision trade-off.**

***Index Terms*—Attenuation Coefficient Estimate, quantitative ultrasound, placenta, regularization**

I. Introduction

Attenuation coefficient estimate (ACE), with its ability to provide microstructural information, is an emerging tool for biological tissue characterization. Successful implementation of ACE to detect fatty liver [1], [2] promises a revolution in the clinical practice for the management of non-alcoholic fatty liver diseases. Recently, ACE is being explored as a potential biomarker to characterize placental tissue and possibly to detect placental disorders [3], [4].

A major limitation of ACE that affects its clinical uptake for these and other applications is the large estimation bias and variance obtained using existing spectral based methods. The main sources of the estimation bias and variance are the presence of inhomogeneities in biological tissue and the fundamental trade-off between ACE resolution and precision. In terms of selecting a homogeneous attenuation estimation region, the placenta, especially when matured, is a particularly challenging organ [4]. In our previous work, we proposed an optimum region-of-interest (AEROI) selection method based on homogeneity indicators such as envelope signal-to-noise ratio deviation. Even with significant improvement (46% reduction compared to the traditional reference phantom method), the resulting intra-subject standard deviation was still as high as 51% of the mean ACE [4].

The sliding window based ACE methods impose a trade-off between image resolution and estimation accuracy and precision. Smaller windows provide high spatial resolution, which is suitable for characterizing the thin (2-3 cm) and heterogeneous placental tissue. However, smaller windows yield noisy and inaccurate ACE measures due to spatial variation noise inherent in ultrasonic scattering [5]. Recent works on regularization attained promising accuracy and precision in ACE measurement without compromising the resolution [6], [7]. However, these methods have not addressed the effect of inhomogeneity, i.e., backscatter variation. The backscatter variation caused by variation in scatterer size and concentration results in a large error in ACE estimation [8].

In this work, we propose a spatially weighted regularization method for ACE measurement, where the degree of regularization would be modulated based on the tissue inhomogeneity information. We evaluate the proposed method using tissue-mimicking phantoms and placenta *ex vivo*.

II. Proposed Method

The ultrasound ACE is a measure of ultrasound amplitude dissipated due to scattering and absorption. To compute ACE according to the reference phantom method (RPM) [9], the data acquired from the tissue is normalized by the data from a well-characterized reference phantom acquired using the same transducer and system settings.

ACE is computed in a $m \times n$ grid using a frequency band discretized at r points. For a RF signal window centered at $(i,j)[i \in (1,m), j \in (1,n)]$ location, the ratio of the power spectrum S from the sample to the reference phantom at frequency $f_k, k \in (1,r)$ can be written as [4]:

$$RS_{i,j,k} = \frac{S^s_{i,j,k}}{S^r_{i,j,k}} = \frac{A^s_{i,j,k}B^s_{i,j,k}}{A^r_{i,j,k}B^r_{i,j,k}} = \frac{e^{-4\alpha^s_{i,j}f_k z_{i,j}}}{e^{-4\alpha^r_{i,j}f_k z_{i,j}}} \cdot \frac{\beta^s_{i,j} f^{n^s_{i,j}}}{\beta^r_{i,j} f^{n^r_{i,j}}}. \quad (1)$$

Here, the s and r superscript denote sample and reference, respectively. A is the total attenuation effect for the axial distance z from the transducer surface to the center of the respective window, B is the backscatter coefficient (BSC), and

978-1-7281-4596-9/19/$31.00 ©2019 IEEE

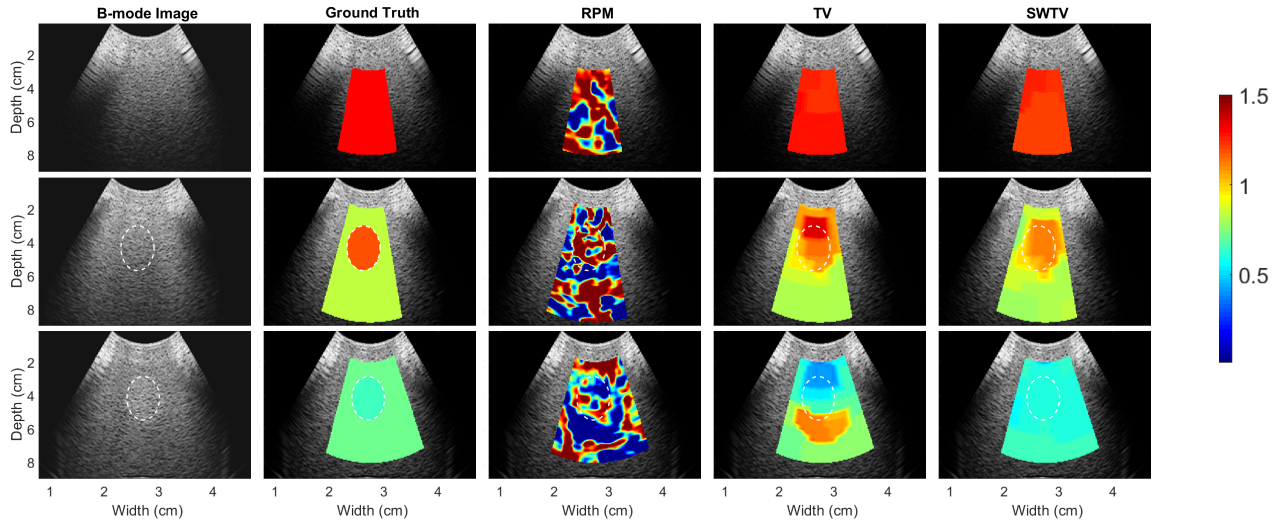

Fig. 1: ACE (dB/cm/MHz) results for CIRS tissue-mimicking phantoms. Top, middle and bottom rows correspond to phantom 1, phantom 2 and phantom 3, respectively. The first two columns show the B-mode images and ground truth ACE overlaid on the B-mode images. The last three columns show ACE maps obtained from the RPM, unweighted TV and SWTV method, respectively. The dashed lines outline the inclusions inside phantom 2 and phantom 3.

α is the effective ACE for the total ultrasound propagation path z. After taking the natural logarithm, (1) reduces to:

$$\ln\left[RS_{i,j,k}\right] = -4(\alpha^s_{i,j} - \alpha^r_{i,j}) f_k z_{i,j} + \ln\frac{\beta^s_{i,j}}{\beta^r_{i,j}} + (n^s_{i,j} - n^r_{i,j}) \ln f. \tag{2}$$

Substituting the following variables in (2) as: $\ln\left[RS_{i,j,k}\right] = Y_{i,j,k}, \alpha^r_{i,j} - \alpha^s_{i,j} = \alpha_{i,j}, \ln\frac{\beta^s_{i,j}}{\beta^r_{i,j}} = \beta_{i,j}, n^s_{i,j} - n^r_{i,j} = n_{i,j}$, we get,

$$Y_{i,j,k} = -4\alpha_{i,j} f_k z_{i,j} + \beta_{i,j} + n_{i,j} \ln f. \tag{3}$$

The above equation can be written in a matrix form: $y = Ax + \eta$, where A, x, and y are given by:

$$\begin{bmatrix} 4z_{1,1}f_1 & \dots & 0 & 1 & \dots & 0 & \ln f_1 & \dots & 0 \\ \vdots & \ddots & \vdots & \vdots & \ddots & \vdots & \vdots & \ddots & \vdots \\ 0 & \dots & 4z_{m,n}f_1 & 0 & \dots & 1 & 0 & \dots & \ln f_1 \\ \vdots & \vdots & \vdots & \vdots & \vdots & \vdots & \vdots & \vdots & \vdots \\ 4z_{1,1}f_r & \dots & 0 & 1 & \dots & 0 & \ln f_r & \dots & 0 \\ \vdots & \ddots & \vdots & \vdots & \ddots & \vdots & \vdots & \ddots & \vdots \\ 0 & \dots & 4z_{m,n}f_r & 0 & \dots & 1 & 0 & \dots & \ln f_r \end{bmatrix}$$

$$y = \begin{bmatrix} Y_{1,1,1} \\ \vdots \\ Y_{m,n,1} \\ \vdots \\ Y_{1,1,r} \\ \vdots \\ Y_{m,n,r} \end{bmatrix}, x = \begin{bmatrix} \alpha_{1,1} \\ \vdots \\ \alpha_{m,n} \\ \beta_{1,1} \\ \vdots \\ \beta_{m,n} \\ n_{1,1} \\ \vdots \\ n_{m,n} \end{bmatrix},$$

and η denotes Gaussian noise with zero mean and standard deviation σ. We propose to solve the following spatially weighted optimization problem for the reconstruction of $x = [\alpha, \beta, n]$ from the noisy estimation Y :

$$\begin{aligned} \hat{x} = \arg\min_x \{ \|(y - Ax)\|_2^2 + \lambda_1 TV(\alpha) \\ + \lambda_2 SWTV(\beta) + \lambda_3 SWTV(n) \}, \end{aligned} \tag{4}$$

where the first term is the data fidelity term, the last three terms are the TV based regularization term, and λ_1, λ_2 and λ_3 are the regularization weights. The TV and SWTV operators are defined as:

$$TV(\alpha) = \sum_{i,j} |\alpha_{i+1,j} - \alpha_{i,j}| + |\alpha_{i,j+1} - \alpha_{i,j}|;$$

$$SWTV(\beta) = \sum_{i,j} W^{i,j} (|\beta_{i+1,j} - \beta_{i,j}| + |\beta_{i,j+1} - \beta_{i,j}|);$$

$$SWTV(n) = \sum_{i,j} W^{i,j} (|n_{i+1,j} - n_{i,j}| + |n_{i,j+1} - n_{i,j}|).$$

Solving (4) will give the values α, the effective ACE for the total ultrasound propagation path. Then the local ACE can be computed as:

$$\alpha^{local}_{i,j} = \frac{\alpha_{i,j} z_{i,j} - \alpha_{i-1,j} z_{i-1,j}}{z_{i,j} - z_{i-1,j}}.$$

In the proposed optimization problem, a spatially weighted total variation (SWTV) regularization has been applied on the BSC terms, β and n. A change in scattering causes larger variation in the BSC terms compared to the ACE. For the regions associated with changes in backscatter, β and n should be lightly regularized to decrease the penalty on their variation. Envelope SNR deviation, ΔSNR_e has previously been used as a criterion to indicate inhomogeneity, i.e., variation in

TABLE I: Ground truth and performance metrics of ACE measures obtained using reference phantom method (RPM), unweighted total variation (TV) and spatially weighted total variation (SWTV) methods for CIRS tissue mimicking phantoms.

Phantom	Ground Truth (dB/cm/MHz)	Mean Absolute Error (%)			Standard Deviation (%)		
		RPM	TV	SWTV	RPM	TV	SWTV
1	1.3	47.58	**2.64**	5.89	58.72	1.57	**1.19**
2 (Background)	0.84	106.38	10.50	**7.20**	134.88	16.11	**10.52**
2 (Inclusion)	1.18	55.07	**8.67**	8.96	75.07	9.47	**4.04**
3 (Background)	0.72	103.50	19.23	**15.58**	132.0	26.07	**12.13**
3 (Inclusion)	0.65	74.92	20.97	**10.23**	87.96	28.27	**5.01**

backscatter [4]. We propose a spatially weighted matrix, W as a function of ΔSNR_e, to adaptively regularize the BSC parameters:

$$W(\Delta SNR_e) = \frac{a}{1 + \exp[b.(\Delta SNR_e - \Delta SNR_e^{\min})]}, \quad (5)$$

where a and b are constants. $\Delta SNR_e^{\min}$ is a nominal ΔSNR_e value indicating the corresponding region to be homogeneous. When $\Delta SNR_e << \Delta SNR_e^{\min}$, the weighting has little effect on the regularization. As ΔSNR_e increases, W decreases resulting in relaxation of the regularization effect on the BSC terms.

III. Experiments and Results

We implemented the proposed SWTV method in MATLAB 2018a (The MathWorks Inc., Natick, MA, USA). The performance of the proposed method was validated on tissue-mimicking phantoms. We also evaluated our method on placenta *ex vivo*. We compare the results obtained from SWTV method with those obtained from RPM and unweighted TV methods. We report the mean absolute error and standard deviation of the error as the metric for bias and variance of computed ACE. Additionally, we report the contrast-to-noise ratio, computed as [6], for phantom 2. We set $\lambda_1 = 2^1, \lambda_2 = 2^{1.5}, \lambda_3 = 2^2$ for the regularization weights.

A. Tissue Mimicking Phantoms: Validation

Ultrasound data were acquired from three custom-built phantoms. Phantom 1 has uniform ACE and uniform BSC, phantom 2 has an inclusion with higher ACE and similar BSC compared to the background, and phantom 3 has an inclusion with higher BSC and similar ACE compared to the background. The ACE ground truth values reported by CIRS (Norfolk, VA, USA) have been shown in Table I and in the second row of Fig. 1. Ultrasound radio-frequency data were acquired from these phantoms using an Ultrasonix SonixTouch machine (Analogic, Canada) and an m4DC7-3 curved array transducer operated at 3.33 MHz. The depth was set to 15 cm with a focus at 10 cm. We select the size of sliding windows to be 6 scanlines (5λ) laterally and 300 radio-frequency samples (25λ) axially, where λ denotes the wavelength. For the reference phantom data, ultrasound data were acquired from a uniform ACE and uniform BSC region with an ACE value of 0.54 dB/cm/MHz with the same system setting.

The resulting ACE maps obtained from RPM, unweighted TV and SWTV methods are shown in Fig. 1 (column 3-5). The

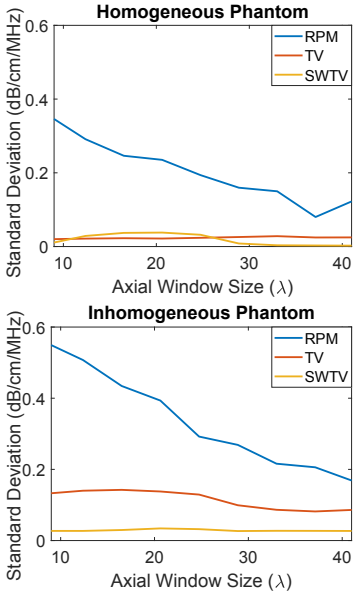

Fig. 2: Effect of window size on precision of ACE measure for phantom 1 (homogeneous phantom) (top) and phantom 3 (inhomogeneous phantom) (bottom).

mean absolute error and standard deviation of the ACE error have been reported in Table I as a percentage of the ground truth values. The high bias and variance obtained from RPM are partly attributed to the insufficient number of independent samples arising from the small window size. Though selecting a larger window size can improve the results from RPM, we select a window size optimum for the regularization based methods and keep the size consistent across the methods for a fair comparison.

For phantom 1 (uniform ACE and uniform BSC), both performance metrics for all the methods are better compared to phantom 2 and phantom 3. This result understates the fact that the ACE measures are more accurate and precise in the homogeneous regions-of-interest.

For phantom 2 (variable ACE and uniform BSC), the contrast-to-noise ratio for ACE maps obtained using the RPM, TV and SWTV methods are 0.31, 1.35, and 2.11, respectively. The inclusion can be distinguished from the ACE maps obtained using both TV and SWTV methods, as opposed to the RPM method. However, the SWTV method improves the contrast-to-noise ratio by 57% compared to that obtained using the unweighted TV method.

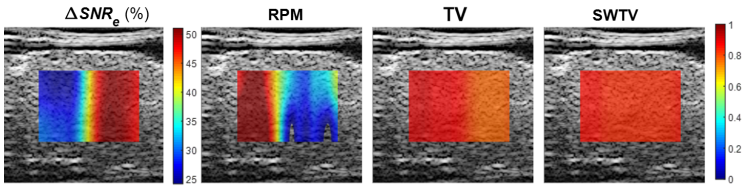

Fig. 3: ΔSNR_e map (left) and ACE maps obtained from the RPM, TV and SWTV methods for a placenta *ex vivo*.

For phantom 3 (Similar ACE and variable BSC), the unweigthed TV method shows underestimation and overestimation of ACE centering at the upper and lower edges of the inclusion, which is a characteristic pattern of ACE error in cases of backscatter variation [8]. However, the ΔSNR_e in this region with backscatter variation is higher than $\Delta SNR_e^{\min}$. Therefore, the proposed method results in improved ACE measure with mean absolute error $< 16\%$ and standard deviation $< 13\%$ by reducing the weight in the inhomogeneous regions.

B. Tissue Mimicking Phantoms: Resolution-Precision Trade-off

To investigate the resolution-precision trade-off in ACE computation, we vary the axial window size from 100 RF samples (8.25λ) to 500 RF samples (41.25λ) for the data acquired with the system setting described in section III-A. The standard deviation of ACE error obtained from phantom 1 (homogeneous phantom) and phantom 3 (inhomogeneous phantom) are shown in Fig. 2. For homogeneous phantom, both TV and SWTV methods attain similar precision for varying resolution, exceeding the resolution-precision trade-off inherent in traditional RPM method. For the inhomogeneous phantom with backscatter variation, however, the TV method shows a similar, though improved, resolution-precision trade-off compared to the RPM. The SWTV method, on the other hand, outperforms both TV and RPM by maintaining similar precision with varying window size.

C. Ex vivo Placenta

For the *ex vivo* placenta, the ultrasound data were acquired using a 4DL14-5/38 4D linear transducer. The depth was set to 3 cm, comparable to the placenta thickness, with a focus at 2 cm. The results for an inhomogeneous region-of-interest (indicated by $mean(\Delta SNR_e) > 20\%$) in placenta is shown in Fig. 3. The mean ACE obtained from the RPM, TV and SWTV methods are 0.77, 0.84 and 0.84 dB/cm/MHz, respectively, whereas the standard deviation is 0.43, 0.05, and 0.01 dB/cm/MHz, respectively. This preliminary *ex vivo* result shows that the proposed SWTV method yields improved precision for ACE measurement in case of the heterogeneous tissue such as placenta.

IV. Conclusion

We present an attenuation coefficient estimation method with improved estimation precision irrespective of resolution and tissue inhomogeneity. For the first time, we incorporate an inhomogeneity indicator into a spatially weighted regularization framework. The approach enables modulating the amount of regularization as a function of the local inhomogeneity. The proposed method outperformed the traditional reference phantom method and unweighted TV method in terms of accuracy, precision and resolution-precision trade-off, whereas the performance improvement was more pronounced in heterogeneous regions with backscatter variation. The ability of the proposed method for precise ACE estimation of thin and heterogeneous tissues shows promise for placental tissue characterization.

Acknowledgment

This work was supported by the Natural Sciences and Engineering Research Council of Canada and the Canadian Institutes of Health Research (Grant CPG-146490). We would like to thank Victoria A. Lessoway and BC Children's Hospital BioBank for the support in ultrasound data acquisition and placenta collection, respectively.

References

[1] F. Deeba, C. Schneider, S. Mohammed, M. Honarvar, E. Tam, R. Rohling, S. Salcudean, "SWTV-ACE: Spatially Weighted Regularization based Attenuation Coefficient Estimation Method for Hepatic Steatosis Detection," in *International Conference on Medical Image Computing and Computer-Assisted Intervention*, Springer, 2019 (*In Press*).

[2] T. Karlas, et al. "Individual patient data meta-analysis of controlled attenuation parameter (CAP) technology for assessing steatosis," *Journal of hepatology*, vol. 66 (5), pp. 1022-1030, 2017.

[3] F. Deeba, M. Ma, M. Pesteie, J. Terry, D. Pugash, J. Hutcheon, C. Mayer, S. Salcudean, R. Rohling, "Multiparametric QUS Analysis for Placental Tissue Characterization," in *Proc. Int. Conf. Eng. Med. Biol. Soc.*, Aug. 2016, pp. 38713874, pp. 3477–3480, IEEE, 2018.

[4] F. Deeba, M. Ma, M. Pesteie, J. Terry, D. Pugash, J. Hutcheon, C. Mayer, S. Salcudean, R. Rohling, "Attenuation Coefficient Estimation of Normal Placentas," *Ultrasound in medicine & biology*, vol. 45 (5), pp. 1081–1093, 2019.

[5] M. L. Oelze, and W. D. O. Jr., "Defining optimal axial and lateral resolution for estimating scatterer properties from volumes using ultrasound backscatter," *J. Acoust. Soc. Am.*, vol. 115 (6), pp. 3226–3234, 2004.

[6] A. L. Coila, and R. Lavarello, "Regularized spectral log difference technique for ultrasonic attenuation imaging," *IEEE Trans. Ultrason., Ferroelectr., Freq. Control*, vol. 65 (3), pp. 378–389, 2018.

[7] Z. Vajihi, et al. "Low Variance Estimation of Backscatter Quantitative Ultrasound Parameters Using Dynamic Programming," *IEEE Trans. Ultrason., Ferroelectr., Freq. Control*, vol. 65 (11), pp. 2042–2053, 2018.

[8] A. D. Pawlicki, and W. D. O. Jr., "Method for estimating total attenuation from a spatial map of attenuation slope for quantitative ultrasound imaging," *Ultrasonic Imaging*, vol. 35 (2), pp. 162–172, 2013.

[9] L. Yao, J. Zagzebski, and E. Madsen, "Backscatter coefficient measurements using a reference phantom to extract depth-dependent instrumentation factors," *Ultrasonic Imaging*, vol.12 (1), pp. 58–70, 1990.